



## Article

# A Carbonized Zeolite/Chitosan Composite as an Adsorbent for Copper (II) and Chromium (VI) Removal from Water

Ender Hidayat <sup>1,2</sup> , Tomoyuki Yoshino <sup>1,2</sup>, Seiichiro Yonemura <sup>1,2</sup>, Yoshiharu Mitoma <sup>1,2</sup>  
and Hiroyuki Harada <sup>1,2,\*</sup> 

<sup>1</sup> Graduate School of Comprehensive and Scientific Research, Prefectural University of Hiroshima, Shobara 727-0023, Japan; hidayatendar1@gmail.com (E.H.); yoshino@pu-hiroshima.ac.jp (T.Y.); yone@pu-hiroshima.ac.jp (S.Y.); mitomay@pu-hiroshima.ac.jp (Y.M.)

<sup>2</sup> Department of Life and Environmental Science, Prefectural University of Hiroshima, Shobara 727-0023, Japan

\* Correspondence: ho-harada@pu-hiroshima.ac.jp

**Abstract:** To address Cu(II) and Cr(VI) water pollution, a carbonized zeolite/chitosan (C-ZLCH) composite adsorbent was produced via pyrolysis at 500 °C for two hours. C-ZLCH was characterized using scanning electron microscopy (SEM), energy-dispersive spectroscopy (EDS), Fourier transform infrared spectroscopy (FTIR), dynamic light scattering (DLS), and zeta potential measurements. The batch experiments were performed by varying the initial pH, concentration, and contact time. The optimal pH values for Cu(II) and Cr(VI) were 8.1 and 9.6, respectively. The highest adsorption capacities for Cu(II) and Cr(VI) were 111.35 mg/g at 60 min and 104.75 mg/g at 90 min, respectively. The effects of chemicals such as sodium (Na<sup>+</sup>), glucose, ammonium (NH<sub>4</sub><sup>+</sup>), and acid red 88 (AR88) were also studied. Statistical analysis showed that sodium had no significant effect on Cu(II) removal, in contrast to Cr(VI) removal. However, there was a significant effect of the presence of glucose, ammonium, and AR88 on both Cu(II) and Cr(VI) removal. The adsorption isotherm and kinetic models were fitted using Langmuir and pseudo-second-order models for Cu(II) and Cr(VI), respectively.

**Keywords:** adsorption; chitosan; Cu(II) removal; Cr(VI) removal; isotherm studies; kinetic studies; carbonized zeolite/chitosan; zeolite



**Citation:** Hidayat, E.; Yoshino, T.; Yonemura, S.; Mitoma, Y.; Harada, H. A Carbonized Zeolite/Chitosan Composite as an Adsorbent for Copper (II) and Chromium (VI) Removal from Water. *Materials* **2023**, *16*, 2532. <https://doi.org/10.3390/ma16062532>

Academic Editors: Patrick M. Martin, Naceur M'Hamdi and Bochra Bejaoui Kefi

Received: 27 February 2023

Revised: 20 March 2023

Accepted: 21 March 2023

Published: 22 March 2023



**Copyright:** © 2023 by the authors. Licensee MDPI, Basel, Switzerland. This article is an open access article distributed under the terms and conditions of the Creative Commons Attribution (CC BY) license (<https://creativecommons.org/licenses/by/4.0/>).

## 1. Background

The aquatic environment is constantly polluted due to population increases and human activities such as industrialization [1]. Heavy metal contamination, a primary environmental concern, is mainly generated by industrial effluents (electroplating, metal finishing, ceramic, and textile industries), including Cu(II) and Cr(VI). Heavy metal ion decontamination is challenging because of its environmental stability and non-biodegradability. Long-term exposure to toxic heavy metals may cause serious health issues, including brain impairment, anemia, bone abnormalities, and cancer [2]. Therefore, practical approaches for capturing heavy metal pollution are urgently required. Researchers have thoroughly investigated heavy metal removal technologies such as ion exchange [3], chemical precipitation, reduction, electrochemical [4], adsorption [5–7], and membrane separation [8,9]. Of these, adsorption is among the best strategies because it is simple to use, convenient, and inexpensive [10].

A wide range of adsorbent materials, including activated carbon from coconuts [11], olive stones [12], silica composites [13], and African palm fruits [14], have been used to remove heavy metals from water. As a result, research has concentrated on developing biodegradable and natural adsorbents such as chitosan [15]. Chitosan is a cationic biopolymer formed by deacetylation of chitin, the second most prevalent polymer [16]. However, it has some disadvantages including poor recovery, low mechanical strength, swelling, and chemical resistance [17]. Furthermore, because it may dissolve in acidic solutions, chitosan is particularly sensitive to pH, which restricts its application because of

the excessive protonation of its amino groups, thereby reducing its adequate adsorption capacities [18]. Cross-linking compounds such as epichlorohydrin [19–21], attapulgite [22], and glutaraldehyde [23] have been utilized to address these issues.

Zeolites are hydrated aluminosilicate minerals with micropores and strong mechanical resistance, which can be utilized to support the chitosan structure. They were constructed using an interconnected tetrahedral alumina ( $\text{AlO}_4$ ) structure and silica ( $\text{SiO}_4$ ). Some authors have used chitosan/zeolite composites to effectively eliminate pollutants, such as dyes [24,25], ammonium [16], fluoride [26], and heavy metals [27].

However, some researchers have succeeded in improving the mechanical strength of chitosan using hydrothermal [28] and pyrolysis [29] methods. However, pyrolysis is the best option because of its zero waste, high carbon yield, and reduced emissions during processing. In the hydrothermal method, processing takes a long time, has a low carbon yield, is costly to autoclave, and retains the residue during processing. Based on the aforementioned results, the carbonization of zeolite/chitosan (C-ZLCH) by pyrolysis is an appropriate solution to overcome the stability problem of chitosan. Scanning electron microscopy (SEM), energy-dispersive spectroscopy (EDS), Fourier transform infrared spectroscopy (FTIR), dynamic light scattering (DLS), and zeta potential measurements were used to characterize the C-ZLCH. The removal of Cu(II) and Cr(VI) from the water was investigated using adsorption isotherms and kinetics. Cu(II) and Cr(VI) removal was examined in the presence of coexisting chemical substances (organic and inorganic), such as sodium ( $\text{Na}^+$ ), glucose, ammonium ( $\text{NH}_4^+$ ), and acid red 88 (AR88) dye.

## 2. Materials and Methods

### 2.1. Materials and Chemicals

Zeolite (ZL) and chitosan (CH) were supplied by Tosoh Co., Ltd., 4560 Kaisei-Cho, Shunan City, Yamaguchi Prefecture, 746-8501, Japan, and Acros Organics, Belgium, respectively. Sodium hydroxide (NaOH), acetic acid ( $\text{CH}_3\text{COOH}$ ), sodium chloride (NaCl), glucose, ammonium chloride ( $\text{NH}_4\text{Cl}$ ), potassium dichromate ( $\text{K}_2\text{Cr}_2\text{O}_7$ ), copper solution (1000 mg/L), hydrochloric acid (HCl), and Acid Red 88 (AR88) were purchased from Kanto Chemical Co., Inc., Tokyo, Japan.

### 2.2. Synthesis of C-ZLCH

Chitosan (1 g) was mixed with 100 mL of 1%  $\text{CH}_3\text{COOH}$  for 24 h at ambient temperature with a magnetic stirrer (Mag-mixer MG600) (solution A). Solution A (25 mL) was mixed with the zeolite (0.5 g) for two hours at 30 °C. The mixture was incubated for 30 min with 1 M NaOH (25 mL). The mixture was filtered (qualitative paper filter no. 5C), and dried at 60 °C for 48 h (ZLCH). ZLCH was then carbonized in a muffle furnace (FO100, Yamato, Japan) at 500 °C for two hours and cooled in a desiccator for 24 h. The mixture was then ground and sieved. This adsorbent is called C-ZLCH.

### 2.3. Batch Adsorption Experiments

The studies of the adsorption of Cu(II) and Cr(VI) ions were conducted three times, and average results appeared in the figure with a bio-shaker (V-BR-36) at 30 °C. The effects of pH (2.0, 4.3, 6.7, 8.1, and 9.6), initial metal ion [Cu(II) and Cr(VI)] concentrations (10, 15, 20, and 25 mg/L), and contact time (30, 60, 90, 150, 180, 1020, and 1440 min) were evaluated. The adsorbed amount and percent adsorption were calculated using Equations (1) and (2), respectively.

$$m/M_t = \frac{m_0 - m_e}{W} V \quad (1)$$

$$\text{Percent adsorption} = \frac{m_0 - m_e}{m_0} \times 100 \quad (2)$$

where

$m$  is the adsorption capacities (mg/g),

$M_t$  is the adsorption capacities at the time (mg/g),  
 Percent adsorption is the metal ions (Cu(II) and Cr(VI)) removal efficiency (%),  
 $m_0$  is the initial metal concentration (mg/L),  
 $m_e$  is the metal ion equilibrium at the time (mg/L),  
 $W$  is the adsorbent weight (C-ZLCH) (g), and  
 $V$  is the volume solution in the batch (L).

#### 2.4. Characterization

Cu(II) and Cr(VI) ions were determined using a heavy metal test kit with a spectrophotometer (Kyoritsu Chemical-Check Lab., Corp, Yokohama, Japan). The zeta potential was measured using Zetasizer Ver. 7.13, Malvern Panalytical Ltd., Kobe, Japan. The SEM images and elemental distribution of C-ZLCH were analyzed using SEM-EDS (JIED-2300, Shimadzu, Kyoto, Japan). The functional groups of C-ZLCH before and after Cu(II) and Cr(VI) adsorption were analyzed using ATR-FTIR (Thermo Scientific Nicolet iS10, Waltham, MA, USA). Particle size distribution was measured using dynamic light scattering (DLS) (Horiba LB-550, Horiba Advanced Techno, Co., Ltd, Kyoto, Japan). DLS and FTIR spectra were processed using Origin 2022b.

#### 2.5. Statistical Analysis

All the results were documented using Microsoft Excel. The effects of chemicals and dyes on Cu(II) and Cr(VI) removal were examined using a completely randomized design (CRD). Data were analyzed using ANOVA with Tukey's test ( $p \leq 0.05$ ) using Minitab 21.3.1.

### 3. Results and Discussion

#### 3.1. Characteristics of the Adsorbent (C-ZLCH)

Figure 1a,b show the SEM images and EDS spectra of C-ZLCH, respectively. As can be seen that the surface has a rough texture and adhesive surface. The EDS data showed that aluminum and silica were present in the zeolite material at 7.99 wt% and 30.84 wt%, respectively. However, sodium (12.69 wt%) appeared because of the alkaline-treated adsorbent preparation using sodium hydroxide. Figure 1c shows that the surface of C-ZLCH was negatively charged at all pH values from 2 to 10, with an average size of 5.5  $\mu\text{m}$  (Figure 1d).

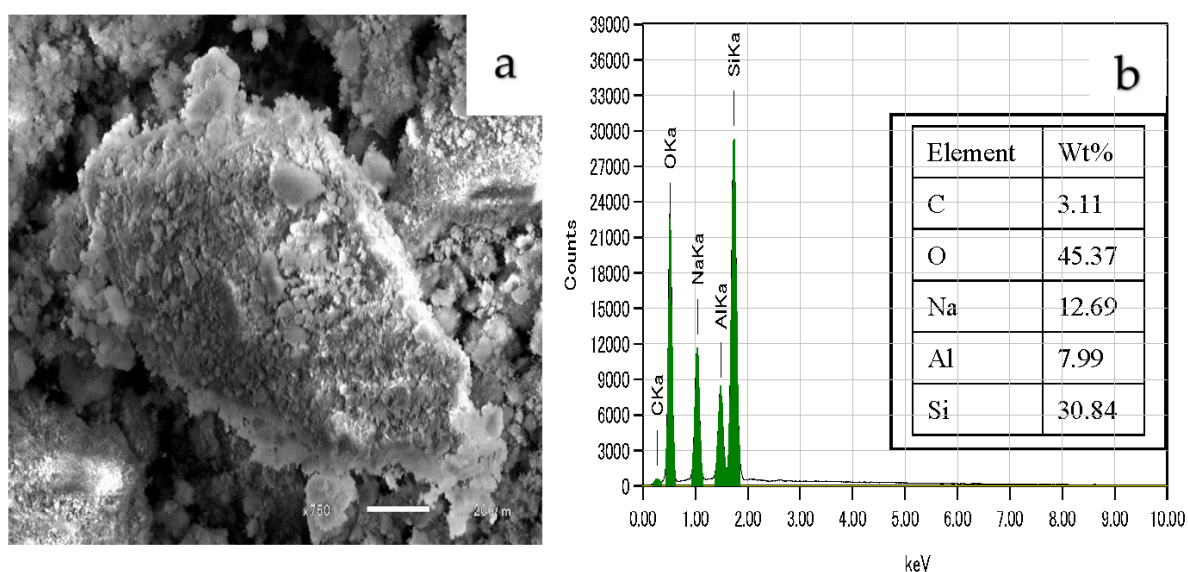
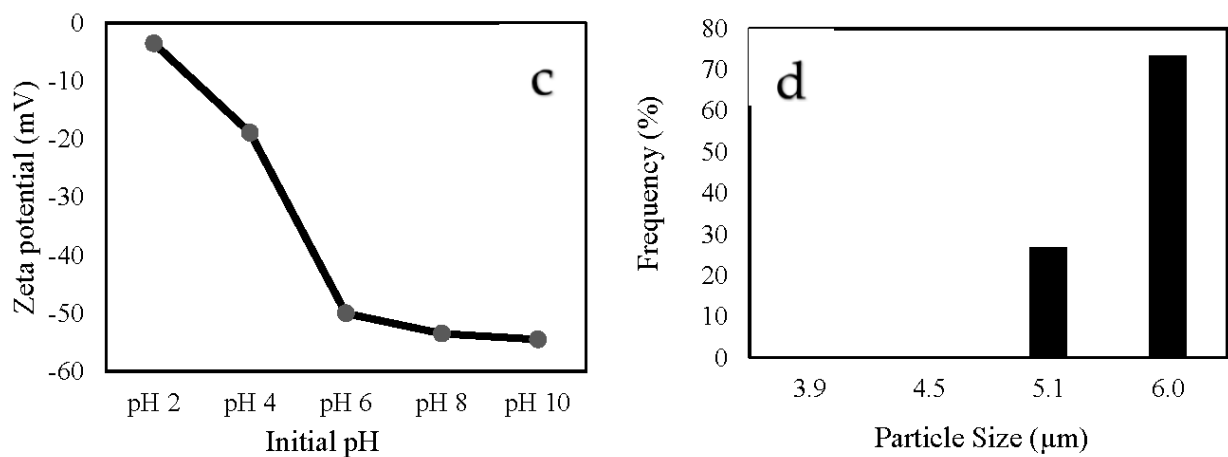


Figure 1. Cont.



**Figure 1.** Characterization of C-ZLCH. (a) SEM photograph. (b) EDS spectra. (c) Zeta potential. (d) Particle size distribution.

### 3.2. FTIR Spectra of C-ZLCH before and after Cu(II) and Cr(VI) Adsorption

The FTIR data for C-ZLCH before and after Cu(II) and Cr(VI) adsorption are shown in Figure 2. The adsorption peaks at  $3338\text{ cm}^{-1}$  increased after Cu(II) and Cr(VI) adsorption at  $3379$  and  $3403\text{ cm}^{-1}$ , respectively. This indicates that the stretching vibrations of  $-\text{OH}$  and  $-\text{NH}$  from chitosan interact with the metal ions [5]. A decrease peak occurred after the Cr(VI) adsorption process from  $1647$  to  $1627\text{ cm}^{-1}$ , which corresponds to carboxylic groups [30], and disappeared after the Cu(II) adsorption process, because carboxyl in acetate species easily decomposes when reacted on copper even at room temperature to evolve  $\text{CO}_2$  as in the thermal reaction [31]. A decrease in the peak intensity after Cu(II) adsorption from  $1455$  to  $1417\text{ cm}^{-1}$  suggests chemical interactions between copper and  $\text{C}-\text{H}$  bending vibrations [32]. The peaks at  $999$  and  $992\text{ cm}^{-1}$  correspond to  $\text{Si}-\text{O}-\text{Si}$  or  $\text{Al}-\text{O}-\text{Al}$  [25]. The peaks at  $702\text{ cm}^{-1}$ ,  $701\text{ cm}^{-1}$ , and  $699\text{ cm}^{-1}$  correspond to the asymmetric vibrations of the  $\text{Si}-\text{O}$  (bridging) and  $\text{Si}-\text{O}$ - (non-bridging) bonds [33].

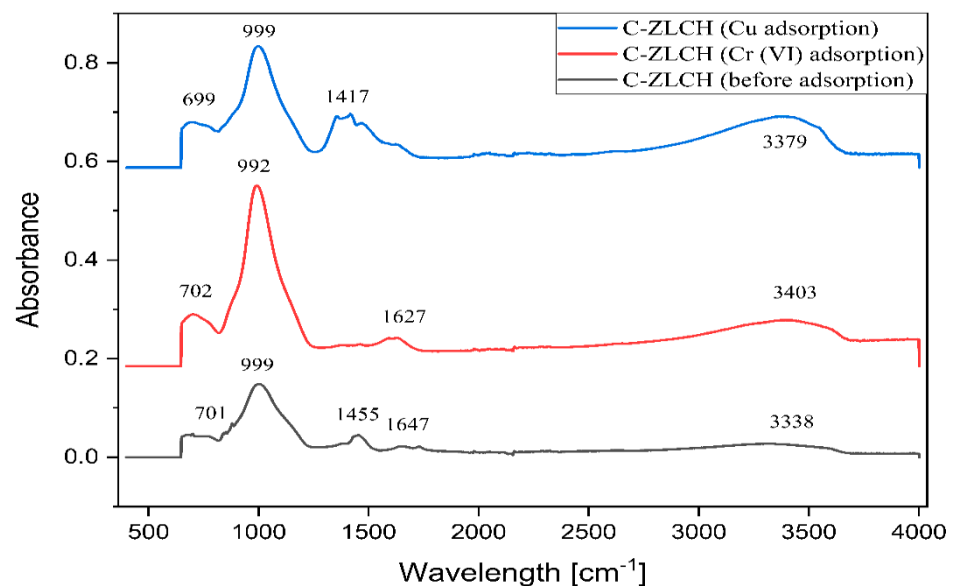


**Figure 2.** FTIR spectra of C-ZLCH before and after Cu(II) and Cr(VI) adsorption.

### 3.3. Initial pH Effects

The pH is the most critical parameter influencing the adsorbate (metal ions) and adsorbent (C-ZLCH) surface charges on Cu(II) and Cr(VI) adsorption [34]. The effect of

pH on Cu(II) and Cr(VI) ion adsorption by C-ZLCH was examined by varying the pH from 2 to 9.6 (Figure 3). The Cu(II) adsorption increased from pH 4.3 to 6.7, reached a peak at pH 8.1, and then decreased slightly to pH 9.6. Negatively charged C-ZLCH surfaces enhanced the removal of Cu(II) via electrostatic interactions. Furthermore,  $\text{Al}^{3+}$  interacts with hydroxyl compounds under alkaline conditions, which is responsible for the cationic exchange between the zeolite and Cu(II) ions in solution [35,36]. Reaction mechanisms in Equation (3).

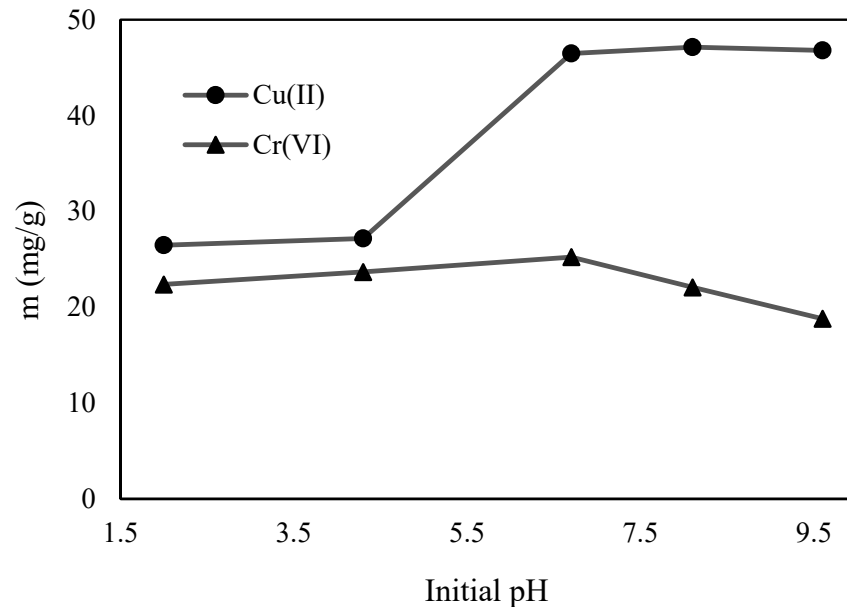
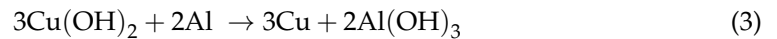


**Figure 3.** Effect of initial pH on Cu(II) and Cr(VI) adsorption. (C-ZLCH: 0.01 g, initial metal ion: 10 mg/L, volume (mL): 50, temperature: 30 °C, and time: 30 min).

Cr(VI) removal peaked at pH 6.7 before dropping to pH 9.6. One possible reason is that under acidic conditions, the hydrogen molecules ( $\text{H}^+$ ) in the solution can dissolve  $-\text{NH}_2$  to form  $\text{NH}_3$  on the surface of C-ZLCH, which increases the exposure of the particle surface active site, thus improving the removal efficiency of Cr(VI). Under alkaline conditions, there is competition between hydroxyl  $-\text{OH}-$  and Cr(VI) species ( $\text{Cr}_2\text{O}_7^{2-}$ ), thus decreasing the adsorption capacities [37,38]. Our findings for Cu(II) and Cr(VI) removal were comparable to those in [39–42].

### 3.4. Initial Concentration Effect

The influence of initial Cu(II) and Cr(VI) concentrations was investigated in the 10–25 mg/L range, 0.01 g/50 mL of C-ZLCH adsorbent, at pH 8.1 and 6.7, respectively. Figure 4 demonstrates that Cu(II) and Cr(VI) adsorption capacities increased from 47.15 to 85.23 mg/g and 25.53 to 31.93 mg/g, respectively. This is because of the high driving force of metal ions and the increase in the number of molecules, which enhances the amount adsorbed onto C-ZLCH [43–47].

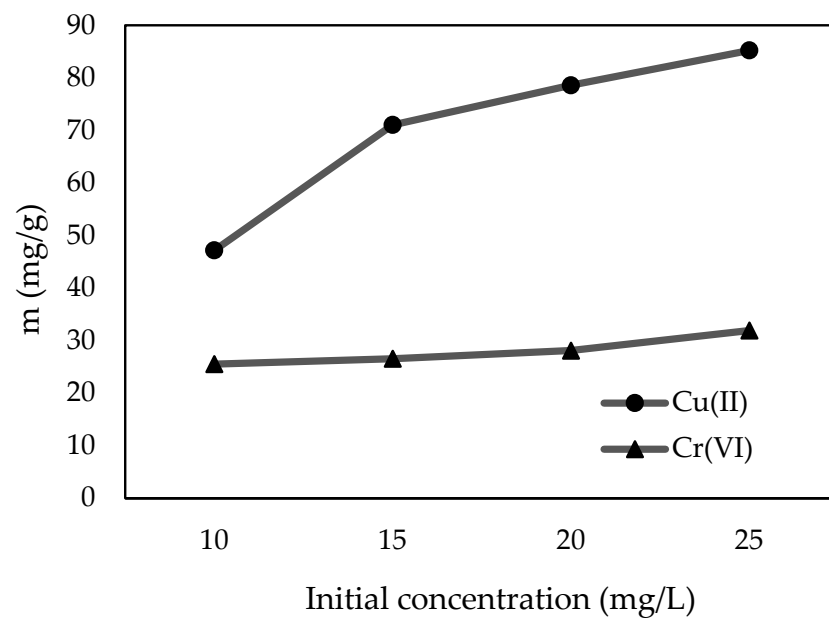


**Figure 4.** Effect of initial concentration on metal ions adsorption. (C-ZLCH: 0.01 g, volume (mL): 50, pH: 8.1 for Cu(II), pH: 6.7 for Cr(VI), temperature: 30 °C, and time: 30 min).

### 3.5. Adsorption Isotherm Studies

Adsorption isotherms are essential for describing the adsorbent capability and interaction between the adsorbate (metal ions) and adsorbent (C-ZLCH). The obtained isotherm parameters are helpful for the proper analysis and design of adsorption systems. The experiment was conducted as follows: 0.01 g was mixed with 50 mL of the metal ion at different initial concentrations, ranging from 10–25 mg/L. The equilibrium concentration of each metal ion was calculated, and the corresponding equilibrium adsorption capacities were obtained. To explore the adsorption process, experimental equilibrium data were evaluated using different isotherm models, including the Langmuir (Equation (4)) and Freundlich (Equation (6)) models [25,40–45].

$$m_e/m = \left( \frac{m_e}{m_{\max}} \right) + 1/(K_1 m_{\max}) \quad (4)$$

$m$  is the amount of the adsorbent (mg/g),  
 $K_1$  is the equilibrium constant of adsorption (L/mg),  
 $m_{\max}$  is the maximal adsorption capacities (mg/g), and  
 $m_e$  is the equilibrium concentration (mg/L).

The essential characteristics of the Langmuir isotherm may be represented in terms of equilibrium, a dimensionless constant also known as the separation factor ( $R_L$ ) in Equation (4).

$$R_L = \left( \frac{1}{1 + b m_0} \right) \quad (5)$$

$m_0$  is the initial concentration (mg/L), and  
 $R_L$  is the separation factor, indicating the adsorption is either  $0 < R_L$  (favorable),  $R_L > 1$  (unfavorable) and  $R_L = 1$  (linear).

The Freundlich model assumes heterogeneous surfaces and multilayer sorption. The linear equation is as follows:

$$\ln m = \ln K_f + \frac{1}{n} \times \ln m_e \quad (6)$$

$K_f$  is the adsorption capacities (mg/g).  
 $1/n$  is the intensity of adsorption.

The isotherm model curves, are shown in Figure 5, and the corresponding fitting results are listed in Table 1. Among the two models, the Langmuir model provided the best fit, because the linear correlation coefficients ( $R^2$ ) were 0.99 and 0.98 for Cu(II) and Cr(VI) adsorption, respectively. More importantly, the Langmuir and Freundlich parameters,  $R_L$  and  $1/n$ , indicate a metal ion adsorption type of  $<1$ . These results suggest favorable Cu(II) and Cr(VI) adsorption.

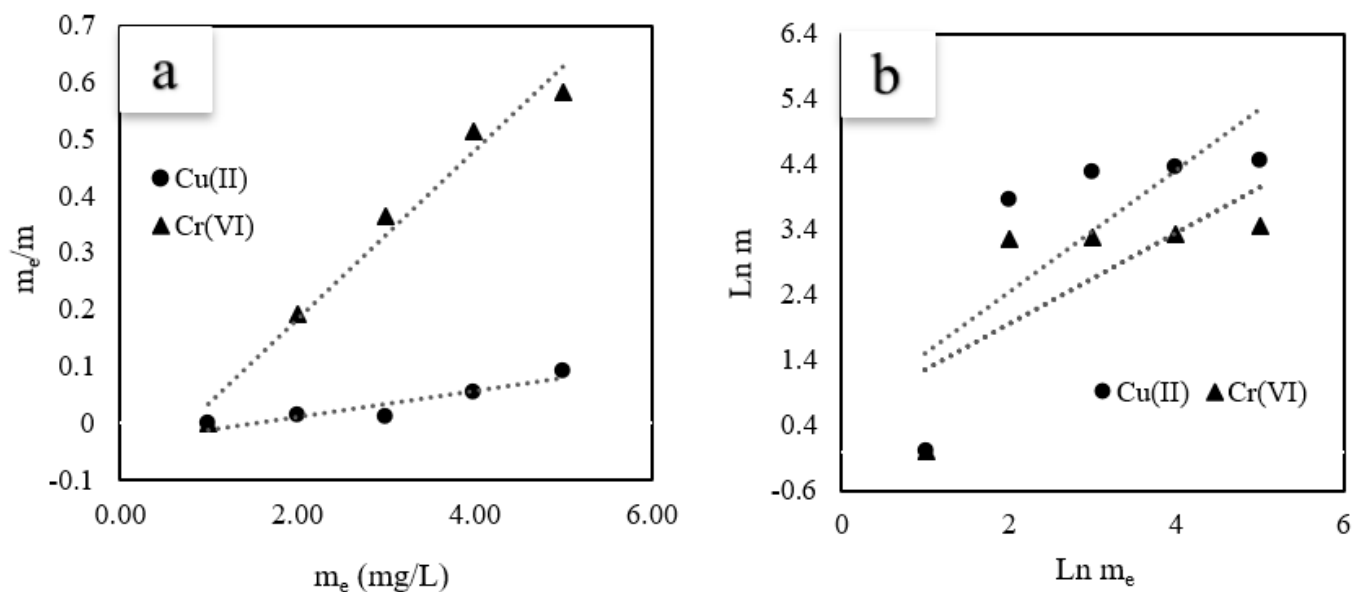


**Figure 5.** Linear curves of adsorption isotherm studies. (a): Langmuir, (b): Freundlich. (C-ZLCH: 0.01 g, volume (mL): 50, pH: 8.1 for Cu(II), 6.7 for Cr(VI), temperature: 30 °C, and time: 30 min).

**Table 1.** Isotherm model parameters for Cu(II) and Cr(VI) adsorption onto C-ZLCH.

Adsorption Isotherm	Isotherm Constant	Metal Ions	
		Cu(II)	Cr(VI)
Langmuir	$m_{\max}$	88.64	34.57
	$K_L$	226.64	14.51
	$R^2$	0.99	0.98
	$R_L$	0.00004	0.00068
Freundlich	$K_f$	13015.09	950.66
	$1/n$	0.17	0.15
	$R^2$	0.70	0.79

### 3.6. Adsorption Kinetic Studies

The effect of time (30–1440 min) on the adsorption capacities of Cu(II) and Cr(VI) was studied. Figure 6 shows that the adsorption capacities of Cu(II) and Cr(VI) increased from 30 to 60 min and then gradually increased up to 90 min for Cr(VI). This is because C-ZLCH contains abundant functional groups (amino, methyl, and hydroxyl groups) and active sites, leading to the rapid adsorption of Cu(II) and Cr(VI). Subsequently, the adsorption capacities decreased and increased for both Cu(II) and Cr(VI) because the adsorption or desorption of metal ions occurred, leading to the reaction [48]. Finally, Cu(II) and Cr(VI) adsorption reached equilibrium at 60 and 90 min with adsorption capacities of 111.35 and 104.75 mg/g, respectively.

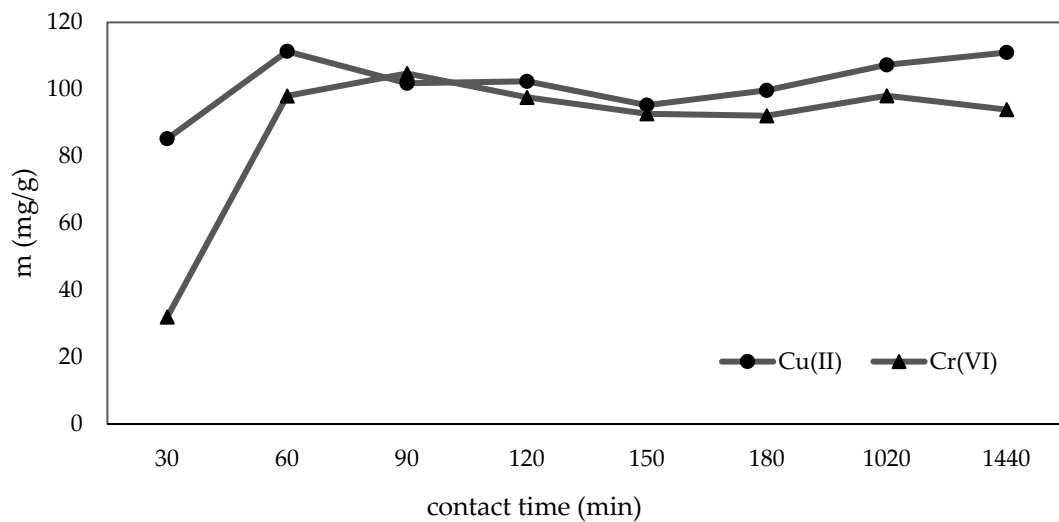


**Figure 6.** Effect of contact time on metal ions adsorption. (C-ZLCH: 0.01 g, volume: 50 mL, metal ions concentration: 25 mg/L, pH: 8.1 for Cu(II), 6.7 for Cr(VI), temperature: 30 °C, and time: 30 min).

Adsorption kinetic studies are indispensable because they can provide information regarding the adsorption mechanism, which is essential for describing process efficiency [25,49,50]. This study used two kinetic models: pseudo-first order (Equation (7)) and pseudo-second order (Equation (8)). The linear form is calculated using the following equation:

$$\log(m - m_t) = \log m - K_1 t \quad (7)$$

$$t/m_t = 1/(K_2 m^2) + t/m \quad (8)$$

where

$K_1$  is the rate constant of pseudo-first-order kinetic model ( $\text{min}^{-1}$ ), and  $K_2$  is the rate constant of pseudo-second-order kinetic model ( $\text{g/mg min}^{-1}$ )  $t$  is the time (min).

The fitting curves of the isotherm models are shown in Figure 7 and the corresponding results are listed in Table 2. As can be seen that the linear correlation coefficient  $R^2$  value of the pseudo-second-order was better than the first-order model for both Cu(II) and Cr(VI). These results indicate that the adsorption rate is controlled by chemical reactions [39,51].

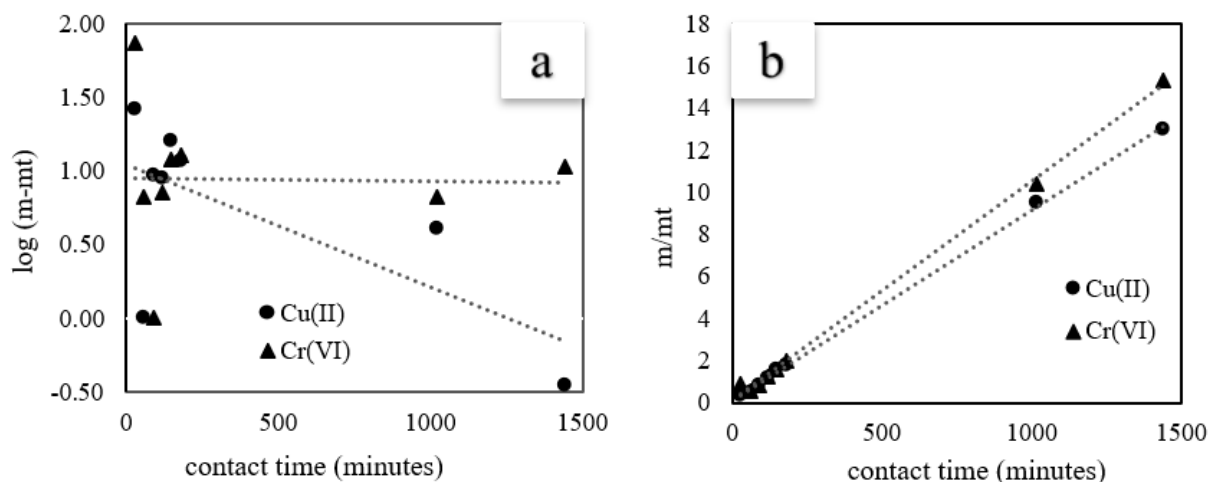


**Figure 7.** Linear curves of adsorption kinetic studies. (a): pseudo-first order, (b): pseudo-second order. (C-ZLCH: 0.01 g, volume: 50 mL, metal ions concentration: 25 mg/L, pH: 8.1 for Cu(II), 6.7 for Cr(VI), temperature: 30 °C).



**Table 2.** Kinetic model parameters for Cu(II) and Cr(VI) adsorption onto C-ZLCH.

Adsorption Kinetic	Parameters	Metal Ion	
		Cu(II)	Cr(VI)
First order	$m_e$	2.83	2.60
	$K_1$	−0.0000133	−0.0000002
	$R^2$	0.4715	0.0003
Second order	$m_e$	111.11	96.15
	$K_2$	0.0007	0.0011
	$R^2$	0.9995	0.9977

### 3.7. Effect of the Presence of Chemical Substances

Many organic and inorganic compounds can affect the adsorption percentage of Cu(II) and Cr(VI) in the environment [52]. This study investigated the effects of Na<sup>+</sup>, glucose, and NH<sub>4</sub><sup>+</sup> at 10 mg/L and 50 mg/L on Cu(II) and Cr(VI) adsorption by C-ZLCH, as shown in Figure 8. Statistical analysis showed that the effect of chemical substances on Cu(II) removal was insignificant, in contrast to Cr(VI) removal. This suggests that Cr(VI) ions compete for binding sites on C-ZLCH [53].

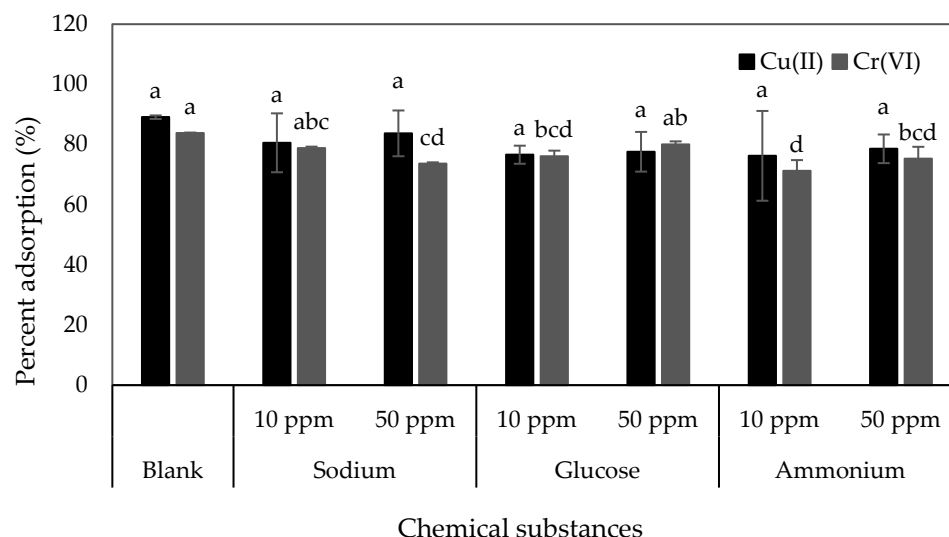


**Figure 8.** Effect of chemical substances on Cu(II) and Cr(VI) adsorption. [Blank: no presence of chemical substances, C-ZLCH: 0.01 g, volume: 50 mL, metal ions concentration: 25 mg/L, pH: 8.1 for Cu(II) at 60 min, pH: 6.7 for Cr(VI) at 90 min, temperature: 30 °C].

### 3.8. Effect of the Presence of AR88 Dye

Industrial waste generally releases heavy metals and dyes, which are major industrial problems [54]. AR88 is a dye that harms humans and the environment, and is possibly trapped in soil [25]. In this study, we investigated the effect of AR88 on the simultaneous removal of metal ions and dyes (Figure 9). The experiment was conducted with optimal Cu(II) and Cr(VI) removal, initial AR88 of 10 mg/L, initial pH 2 and pH 8.1 for Cu(II), and pH 2 and pH 6.7 for Cr(VI). Statistical analysis showed that the presence of AR88 dye had no significant effect on Cu(II) removal. However, it significantly affected Cr(VI) removal at pH 2 compared to the absence of AR88 (blank). This indicates that the highest percentage of adsorption of Cu(II) and Cr(VI) was similar to that in the absence of AR88 dye (Figure 3). Moreover, the highest AR88 removal was observed at pH 2 for both Cu(II) and Cr(VI), similar to the results reported by Hidayat et al. [25].

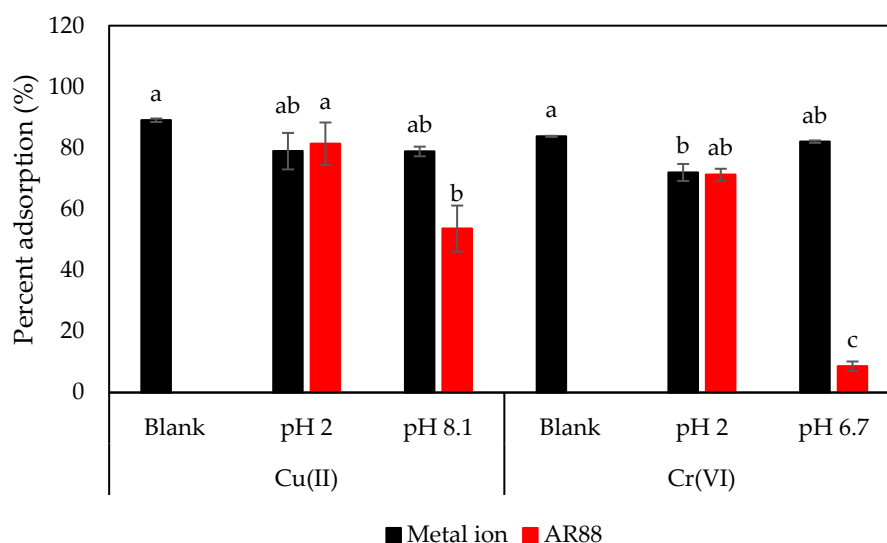


**Figure 9.** Effect of AR88 on Cu(II) and Cr(VI) adsorption. [Blank: no presence of AR88 dye, pH 8.1 for Cu(II) and pH 6.7 for Cr(VI), C-ZLCH: 0.01 g, volume: 50 mL, metal ions concentration: 25 mg/L, pH: 8.1 for Cu(II) at 60 min, pH: 6.7 for Cr(VI) at 90 min, temperature: 30 °C].

### 3.9. Comparison with Other Adsorbents

Table 3 lists the adsorption capacities of different adsorbents. Thus, C-ZLCH is a promising adsorbent for removing Cu(II) and Cr(VI) from water.

**Table 3.** Comparison with other adsorbents.

Adsorbents	m (mg/g)		References
	Cu(II)	Cr(VI)	
Hematite Fe-oxide-coated sand (pH 1)	3.93		[55]
Chitin	2.80		[56]
Magnetite nano-adsorbent (MNA)	4.42		[57]
Fe <sub>2</sub> O <sub>3</sub> -carbon foam	3.8	6.7	[58]
HKUST-1/SiO <sub>2</sub>		62.38	[7]
NH <sub>2</sub> -ASNs		34.0	[59]
NH <sub>2</sub> -MSNs	53.5	42.2	[59]
Fly ash-derived zeolite	92.59		[60]
Fly ash-based zeolite A			[61]
Natural zeolite-coated magnetite		43.93	[62]
Amine-functionalized zeolite		13.5	[63]
Carbonized zeolite/chitosan	111.35	104.75	This study

## 4. Conclusions

A carbonized zeolite/chitosan (C-ZLCH) composite was prepared via pyrolysis to remove Cu(II) and Cr(VI) from water. The results indicated that the pH was optimal at pH 8.1 and 6.7 for Cu(II) and Cr(VI), respectively. Cu(II) and Cr(VI) adsorption capacities were 111.35 and 104.75 mg/g after 60 and 90 min, respectively. For both Cu(II) and Cr(VI), the adsorption isotherm followed the Langmuir model, which is favorable ( $RL$  and  $1/n < 1$ ). The Cu(II) and Cr(VI) kinetic models were fitted to a pseudo-second-order model, which indicated chemical sorption on the C-ZLCH adsorbent. Statistical analysis showed no significant effect on Cu(II) removal in the presence of sodium, in contrast to the presence of glucose, ammonium, and AR88. However, there was a significant effect on Cr(VI) removal in the presence of chemical substances and AR88 dye.

**Author Contributions:** Conceptualization, E.H.; Methodology, E.H.; Validation, Y.M.; Formal analysis, E.H. and H.H.; Investigation, E.H. and T.Y.; Data curation, S.Y.; Writing—original draft, E.H.; Writing—review & editing, E.H.; Visualization, T.Y.; Supervision, S.Y., Y.M. and H.H.; Project administration, H.H. All authors have read and agreed to the published version of the manuscript.

**Funding:** This research received no external funding.

**Data Availability Statement:** Not applicable.

**Acknowledgments:** The author (E.H.) would like to thank the MEXT Scholarship for sponsorship while studying at the Prefectural University of Hiroshima, Japan.

**Conflicts of Interest:** The authors report no competing interest to declare.

## References

1. Lim, J.Y.; Mubarak, N.M.; Abdullah, E.C.; Nizamuddin, S.; Khalid, M.; Inamuddin. Recent trends in the synthesis of graphene and graphene oxide based nanomaterials for removal of heavy metals—A review. *J. Ind. Eng. Chem.* **2018**, *66*, 29–44. [[CrossRef](#)]
2. Usman, T.M.; Xintai, S.; Mengqi, Z.; Yinnian, L.; Ronglan, W.; Dejun, C. Preparation of hydroxypropyl-cyclodextrin-graphene/Fe<sub>3</sub>O<sub>4</sub> and its adsorption properties for heavy metals. *Surf. Interfaces* **2019**, *16*, 43–49. [[CrossRef](#)]
3. Wu, S.; Yan, P.; Yang, W.; Zhou, J.; Wang, H.; Che, L.; Zhu, P. ZnCl<sub>2</sub> enabled synthesis of activated carbons from ion-exchange resin for efficient removal of Cu<sup>2+</sup> ions from water via capacitive deionization. *Chemosphere* **2021**, *264*, 128557. [[CrossRef](#)] [[PubMed](#)]
4. Zhang, H.; Zhu, J.; Ma, L.; Kang, L.; Hu, M.; Li, S.; Chen, Y. Electrochemical Adsorption of Cs<sup>+</sup> Ions on H-Todorokite Nanorods. *ACS Omega* **2020**, *5*, 1062–1067. [[CrossRef](#)] [[PubMed](#)]
5. Zhang, S.; Zhang, Y.; Fu, L.; Jing, M. A chitosan fiber as green material for removing Cr(VI) and Cu(II) ions pollutants. *Sci. Rep.* **2021**, *11*, 22942. [[CrossRef](#)] [[PubMed](#)]
6. Masoumi, H.; Ghaemi, A.; Gilani, H.G. Evaluation of hyper-cross-linked polymers performances in the removal of hazardous heavy metal ions: A review. *Sep. Purif. Technol.* **2021**, *260*, 118221. [[CrossRef](#)]
7. Feng, S.; Ni, J.; Li, S.; Cao, X.; Gao, J.; Zhang, W.; Chen, F.; Huang, R.; Zhang, Y.; Feng, S. Removal of hexavalent chromium by electrospun silicon dioxide nanofibers embedded with copper-based organic frameworks. *Sustainability* **2022**, *14*, 13780. [[CrossRef](#)]
8. Islam, M.S.; Vogler, R.J.; Hasnine, S.M.A.A.; Hernández, S.; Malekzadeh, N.; Hoelen, T.P.; Hatakeyama, E.S.; Bhattacharyya, D. Mercury removal from wastewater using cysteamine functionalized membranes. *ACS Omega* **2020**, *5*, 22255–22267. [[CrossRef](#)]
9. Hamid, S.A.; Shahadat, M.; Ballinger, B.; Azha, S.F.; Ismail, S.; Ali, S.W.; Ahammad, S.Z. Role of clay-based membrane for removal of copper from aqueous solution. *J. Saudi. Chem. Soc.* **2020**, *24*, 785–798. [[CrossRef](#)]
10. Huang, R.Y.; He, L.; Zhang, T.; Li, D.Q.; Tang, P.G.; Feng, Y.J. Novel carbon paper@magnesium silicate composite porous films: Design, fabrication, and adsorption behavior for heavy metal ions in aqueous solution. *ACS Appl. Mater. Int.* **2018**, *10*, 22776–22785. [[CrossRef](#)]
11. Yang, K.; Peng, J.; Srinivasakannan, C.; Zhang, L.; Xia, H.; Duan, X. Preparation of high surface area activated carbon from coconut shells using microwave heating. *Bioresour. Technol.* **2010**, *101*, 6163–6169. [[CrossRef](#)] [[PubMed](#)]
12. Saleem, J.; Shahid, U.B.; Hijab, M.; Mackey, H.; McKay, G. Production and applications of activated carbons as adsorbents from olive stones. *Biomass. Convers. Biorefin.* **2019**, *9*, 775–802. [[CrossRef](#)]
13. Karnib, M.; Kabbani, A.; Holail, H.; Olama, Z. Heavy metals removal using activated carbon, silica and silica activated carbon composite. *Energy Procedia* **2014**, *50*, 113–120. [[CrossRef](#)]
14. Abdulrazak, S.; Hussaini, K.; Sani, H.M. Evaluation of removal efficiency of heavy metals by low-cost activated carbon prepared from African palm fruit. *Appl. Water Sci.* **2017**, *7*, 3151–3155. [[CrossRef](#)]
15. Pu, S.; Hui, M.; Zinchenko, A.; Chu, W. Novel highly porous magnetic hydrogel beads composed of chitosan and sodium citrate: An effective adsorbent for the removal of heavy metals from aqueous solution. *Environ. Sci. Pollut. Res.* **2017**, *24*, 16520–16530. [[CrossRef](#)] [[PubMed](#)]
16. Yang, K.; Zhang, X.; Chao, C.; Zhang, B.; Liu, J. In-situ preparation of NaA zeolite/chitosan porous hybrid beads for removal of ammonium from aqueous solution. *Carbohydr. Polym.* **2014**, *107*, 103–109. [[CrossRef](#)]
17. Habibi, U.; Siddique, T.A.; Joo, T.C.; Salleh, A.; Ang, B.C.; Afifi, A.M. Synthesis of chitosan/polyvinyl alcohol/zeolite composite for removal of methyl orange, congo red and chromium (VI) by flocculation/adsorption. *Carbohydr. Polym.* **2017**, *157*, 1568–1576. [[CrossRef](#)]
18. Dash, M.; Chiellini, F.; Ottenbrite, R.M.; Chiellini, E. Chitosan—A versatile semi-synthetic polymer in biomedical applications. *Prog. Polym. Sci.* **2011**, *36*, 981–1014. [[CrossRef](#)]
19. Ngah, W.S.W.; Endud, C.S.; Mayanar, R. Removal of copper(II) ions from aqueous solution onto chitosan and cross-linking chitosan beads. *React. Funct. Polym.* **2002**, *20*, 181–190. [[CrossRef](#)]
20. Tirtom, V.N.; Dinçer, A.; Becerik, S.; Aydemir, T.; Çelik, A. Comparative adsorption of Ni(II) and Cd(II) ions on epichlorohydrin crosslinked chitosan–clay composite beads in aqueous solution. *Chem. Eng. J.* **2012**, *197*, 379–386. [[CrossRef](#)]
21. Thinh, N.N.; Hanh, P.T.B.; Ha, L.T.T.; Anh, L.N.; Hoang, T.V.; Hoang, V.D.; Dang, L.H.; Khoi, N.V.; Lam, T.D. Magnetic chitosan nanoparticles for removal of Cr(VI) from aqueous solution. *Mater. Sci. Eng. C* **2013**, *33*, 1214–1218. [[CrossRef](#)] [[PubMed](#)]

22. Deng, Y.; Wang, L.; Hu, X.; Liu, B.; Wei, Z.; Yang, S.; Sun, C. Highly efficient removal of tannic acid from aqueous solution by chitosan-coated attapulgite. *Chem. Eng. J.* **2012**, *181–182*, 300–306. [[CrossRef](#)]
23. Galan, J.; Trilleras, J.; Zapata, P.A.; Arana, V.A.; Tovar, C.D.G. Optimization of chitosan glutaraldehyde-crosslinked beads for reactive blue 4 anionic dye removal using a surface response methodology. *Life* **2021**, *11*, 85. [[CrossRef](#)] [[PubMed](#)]
24. Khanday, W.A.; Asif, M.; Hameed, B.H. Cross-linked beads of activated oil palm ash zeolite/chitosan composite as a bio-adsorbent for the removal of methylene blue and acid blue 29 dyes. *Int. J. Biol. Macromol.* **2017**, *95*, 895–902. [[CrossRef](#)] [[PubMed](#)]
25. Hidayat, E.; Harada, H.; Mitoma, Y.; Yonemura, S.; Halem, A.I.D. Rapid removal of acid red 88 by zeolite/chitosan hydrogel in aqueous solution. *Polymers* **2022**, *14*, 893. [[CrossRef](#)] [[PubMed](#)]
26. Orozco, J.A.A.; Rojas, A.I.F.; Mendez, J.R.R.; Flores, P.E.D. Synergistic effect of zeolite/chitosan in the removal of fluoride from aqueous solution. *Environ. Technol.* **2018**, *41*, 1554–1567. [[CrossRef](#)]
27. Zhang, Y.; Yan, W.; Sun, Z.; Pan, C.; Mi, X.; Zhao, G.; Gao, J. Fabrication of porous zeolite/chitosan monoliths and their applications for drug release and metal ions adsorption. *Carbohydr. Polym.* **2015**, *117*, 657–665. [[CrossRef](#)]
28. Hammi, N.; Chen, S.; Dumeignil, F.; Royer, S.; Kadib, A.E. Chitosan as a sustainable precursor for nitrogen-containing carbon nanomaterials: Synthesis and uses. *Mater. Today Sustain.* **2020**, *10*, 100053. [[CrossRef](#)]
29. Bengisu, M.; Yilmaz, E. Oxidation and pyrolysis of chitosan as a route for carbon fiber derivation. *Carbohydr. Polym.* **2002**, *50*, 165–175. [[CrossRef](#)]
30. Fajardo, A.R.; Lopes, L.C.; Pereira, A.G.B.; Rubira, A.F.; Muniz, E.C. Polyelectrolyte complexes based on pectin-NH<sub>2</sub> and chondroitin sulfate. *Carbohydr. Polym.* **2012**, *87*, 1950–1955. [[CrossRef](#)]
31. Rana, R.; Bavisotto, R.; Hou, K.; Tysoe, W.T. Surface chemistry at the solid-solid interface: Mechanically induced reaction pathways of C<sub>8</sub> carboxyl acid monolayers on copper. *Phys. Chem. Chem. Phys.* **2021**, *23*, 17803–17812. [[CrossRef](#)] [[PubMed](#)]
32. Bhanja, P.; Mishra, S.; Manna, K.; Saha, K.D.; Bhaumik, A. Porous polymer bearing polyphenolic organic building units as a chemotherapeutic agent for cancer treatment. *ACS Omega* **2018**, *3*, 529–535. [[CrossRef](#)]
33. Awuah, B.K.; Kiti, E.V.; Nkrumah, I.; Ikyreve, R.E.; Radecka, I.; Williams, C. Parametric, equilibrium, and kinetic study of the removal of salt ions from Ghanaian seawater by adsorption onto zeolite X. *Desalin. Water Treat.* **2016**, *57*, 21654–21663. [[CrossRef](#)]
34. Lu, J.; Li, B.; Li, W.; Zhang, X.; Zhang, W.; Zhang, P.; Su, R.; Liu, D. Nano iron oxides impregnated chitosan beads towards aqueous Cr(VI) elimination: Components optimization and performance evaluation. *Colloids Surf. A Physicochem. Eng. Asp.* **2021**, *625*, 126902. [[CrossRef](#)]
35. Sun, X.; Guo, P.; Sun, Y.; Cui, Y. Adsorption of hexavalent chromium by sodium alginate fiber biochar loaded with lanthanum. *Materials* **2021**, *14*, 2224. [[CrossRef](#)] [[PubMed](#)]
36. Mandal, S.; Sahu, M.K.; Giri, A.K.; Patel, R.K. Adsorption studies of chromium (VI) removal from water by lanthanum diethanolamine hybrid material. *Environ. Technol.* **2014**, *35*, 817–832. [[CrossRef](#)] [[PubMed](#)]
37. Shih, Y.H.; Hsu, C.Y.; Su, Y.F. Reduction of hexachlorobenzene by nanoscale zero-valent iron: Kinetics, pH effect, and degradation mechanism. *Sep. Purif. Technol.* **2011**, *76*, 268–274. [[CrossRef](#)]
38. Kumar, A.; Jena, H.M. Adsorption of Cr(VI) from aqueous phase by high surface area activated carbon prepared by chemical activation with ZnCl<sub>2</sub>. *Process. Saf. Environ. Prot.* **2017**, *109*, 63–71. [[CrossRef](#)]
39. Guo, T.; Bulin, C.; Ma, Z.; Li, B.; Zhang, Y.; Zhang, B.; Xing, R.; Ge, X. Mechanism of Cd(II) and Cu(II) adsorption onto few-layered magnetic graphene oxide as an efficient adsorbent. *ACS Omega* **2021**, *6*, 16535–16545. [[CrossRef](#)]
40. Benzaoui, T.; Selatnia, A.; Djabali, D. Adsorption of copper (II) ions from aqueous solution using bottom ash of expired drugs incineration. *Adsorp. Sci. Technol.* **2018**, *36*, 114–129. [[CrossRef](#)]
41. Li, L.; Cao, G.; Zhu, R. Adsorption of Cr(VI) from aqueous solution by a litchi shell-based adsorbent. *Environ. Res.* **2021**, *196*, 110356. [[CrossRef](#)] [[PubMed](#)]
42. Qi, J.; Li, B.; Zhou, P.; Su, X.; Yang, D.; Wu, J.; Wang, Z.; Liang, X. Study on adsorption of hexavalent chromium by composite material prepared from iron-based solid wastes. *Sci. Rep.* **2023**, *13*, 135. [[CrossRef](#)] [[PubMed](#)]
43. Hidayat, E.; Yonemura, S.; Mitoma, Y.; Harada, H. Methylene blue removal by chitosan cross-linked zeolite from aqueous solution and other ion effects: Isotherm, kinetic, and desorption studies. *Adsorp. Sci. Technol.* **2022**, *1853758*, 10. [[CrossRef](#)]
44. Hidayat, E.; Khaekhum, S.; Yonemura, S.; Mitoma, Y.; Harada, H. Biosorption of eriochrome black T using *Exserohilum rostratum* NMS1.5 mycelia biomass. *J* **2022**, *5*, 427–434. [[CrossRef](#)]
45. Hidayat, E.; Yoshino, T.; Yonemura, S.; Mitoma, Y.; Harada, H. Synthesis, adsorption isotherm and kinetic study of alkaline-treated zeolite/chitosan/Fe<sup>3+</sup> composites for nitrate removal from aqueous solution—Anion and dye effects. *Gels* **2022**, *8*, 782. [[CrossRef](#)]
46. Ajmani, A.; Shahnaz, T.; Subbiah, S.; Narayanasamy, S. Hexavalent chromium adsorption on virgin, biochar, and chemically modified carbons prepared from *Phanera vahlii* fruit biomass: Equilibrium, kinetics, and thermodynamics approach. *Environ. Sci. Pollut. Res.* **2019**, *26*, 32137–32150. [[CrossRef](#)] [[PubMed](#)]
47. Moussavi, G.; Barikbin, B. Biosorption of chromium(VI) from industrial wastewater onto pistachio hull waste biomass. *Chem. Eng. J.* **2010**, *162*, 893–900. [[CrossRef](#)]
48. Nekhunguni, P.M.; Tavengwa, N.T.; Tutu, H. Sorption of uranium(VI) onto hydrous ferric oxide-modified zeolite: Assessment of the effect of pH, contact time, temperature, selected cations and anions on sorbent interactions. *J. Environ. Manag.* **2017**, *204*, 571–582. [[CrossRef](#)] [[PubMed](#)]
49. Degefu, D.M.; Dawit, M. Chromium removal from Modjo Tannery wastewater using *Moringa stenopetala* seed powder as an adsorbent. *Water Air Soil Pollut.* **2013**, *224*, 1719. [[CrossRef](#)]

50. Jembere, A.L.; Genet, M.B. Comparative adsorptive performance of adsorbents developed from sugar industrial wastes for the removal of melanoidin pigment from molasses distillery spent wash. *Water Resour. Ind.* **2021**, *26*, 100165. [[CrossRef](#)]
51. Ho, Y.S.; McKay, G. Pseudo-second order model for sorption processes. *Process Biochem.* **1999**, *34*, 451–465. [[CrossRef](#)]
52. Song, L.; Feng, Y.; Zhu, C.; Liu, F.; Li, A. Enhanced synergistic removal of Cr(VI) and Cd(II) with bi-functional biomass-based composites. *J. Hazard. Mater.* **2020**, *388*, 121776. [[CrossRef](#)] [[PubMed](#)]
53. Hamadeen, H.M.; Elkhatib, E.A.; Moharem, M.L. Optimization and mechanisms of rapid adsorptive removal of chromium (VI) from wastewater using industrial waste derived nanoparticles. *Sci. Rep.* **2022**, *12*, 14174. [[CrossRef](#)] [[PubMed](#)]
54. Stagnaro, S.M.; Volzone, C.; Huck, L. Nanoclay as adsorbent: Evaluation for removing dyes used in the textile industry. *Procedia Mater. Sci.* **2015**, *8*, 586–591. [[CrossRef](#)]
55. Khan, J.; Lin, S.; Nizeyimana, J.C.; Wu, Y.; Wang, Q.; Liu, X. Removal of copper ions from wastewater via adsorption on modified hematite ( $\alpha\text{-Fe}_2\text{O}_3$ ) iron oxide coated sand. *J. Clean. Prod.* **2021**, *319*, 128687. [[CrossRef](#)]
56. Boulaiche, W.; Hamdi, B.; Trari, M. Removal of heavy metals by chitin: Equilibrium, kinetic and thermodynamic studies. *Appl. Water. Sci.* **2019**, *9*, 39. [[CrossRef](#)]
57. Sulaiman, S.; Azis, R.S.; Ismail, I.; Man, H.C.; Yusof, K.F.M.; Abba, M.U.; Katibi, K.K. Adsorptive removal of copper (II) ions from aqueous solution using a magnetite nano-adsorbent from mill scale waste: Synthesis, characterization, adsorption and kinetic modelling studies. *Nanoscale Res. Lett.* **2021**, *16*, 168. [[CrossRef](#)]
58. Lee, C.G.; Lee, S.; Park, J.A.; Park, C.; Lee, S.J.; Kim, S.B.; An, B.; Yun, S.T.; Lee, S.H.; Choi, J.W. Removal of copper, nickel and chromium mixtures from metal plating wastewater by adsorption with modified carbon foam. *Chemosphere* **2017**, *166*, 203–211. [[CrossRef](#)]
59. Jang, E.H.; Pack, S.P.; Kim, I.; Chung, S. A systematic study of hexavalent chromium adsorption and removal from aqueous environments using chemically functionalized amorphous and mesoporous silica nanoparticles. *Sci. Rep.* **2020**, *10*, 5558. [[CrossRef](#)]
60. Buema, G.; Trifas, L.M.; Harja, M. Removal of toxic copper ion from aqueous media by adsorption on fly ash-derived zeolites: Kinetic and equilibrium studies. *Polymers* **2021**, *13*, 3468. [[CrossRef](#)]
61. Paramitha, T.; Wulandari, W.; Rizkiana, J.; Sasongko, D. Performance evaluation of coal fly ash based zeolite a for heavy metal ions adsorption of wastewater. *IOP Conf. Ser. Mat. Sci. Eng.* **2019**, *543*, 012095. [[CrossRef](#)]
62. Asanu, M.; Beyene, D.; Befekadu, A. Removal of hexavalent chromium from aqueous solutions using natural zeolite coated with magnetite nanoparticles: Optimization, kinetics, and equilibrium studies. *Adsorp. Sci. Technol.* **2022**, *8625489*, 22. [[CrossRef](#)]
63. Nasanjargal, S.; Munkhpurev, B.A.; Kano, N.; Kim, H.J.; Ganchimeg, Y. The removal of chromium(VI) from aqueous solution by amine-functionalized zeolite: Kinetics, thermodynamics, and equilibrium study. *J. Environ. Prot.* **2021**, *12*, 654–675. [[CrossRef](#)]

**Disclaimer/Publisher's Note:** The statements, opinions and data contained in all publications are solely those of the individual author(s) and contributor(s) and not of MDPI and/or the editor(s). MDPI and/or the editor(s) disclaim responsibility for any injury to people or property resulting from any ideas, methods, instructions or products referred to in the content.